



## Potential of MEMS technologies for manufacturing of high-fidelity microspeakers

Elie Lefeuvre, Iman Shahosseini, Johan Moulin, Marion Woytasik, Emile Martincic, Guy Lemarquand, Eric Sturtzer, Gaël Pillonnet

### ► To cite this version:

Elie Lefeuvre, Iman Shahosseini, Johan Moulin, Marion Woytasik, Emile Martincic, et al.. Potential of MEMS technologies for manufacturing of high-fidelity microspeakers. Acoustics 2012, Apr 2012, Nantes, France. hal-00811084

**HAL Id: hal-00811084**

**<https://hal.science/hal-00811084>**

Submitted on 23 Apr 2012

**HAL** is a multi-disciplinary open access archive for the deposit and dissemination of scientific research documents, whether they are published or not. The documents may come from teaching and research institutions in France or abroad, or from public or private research centers.

L'archive ouverte pluridisciplinaire **HAL**, est destinée au dépôt et à la diffusion de documents scientifiques de niveau recherche, publiés ou non, émanant des établissements d'enseignement et de recherche français ou étrangers, des laboratoires publics ou privés.



# ACOUSTICS 2012

## Potential of MEMS technologies for manufacturing of high-fidelity microspeakers

E. Lefeuvre<sup>a</sup>, I. Shahosseini<sup>a</sup>, J. Moulin<sup>a</sup>, M. Woytasik<sup>a</sup>, E. Martincic<sup>a</sup>, G. Lemarquand<sup>b</sup>, E. Sturtzer<sup>c</sup> and G. Pillonnet<sup>c</sup>

<sup>a</sup>Institut d'électronique fondamentale, bat. 220 Av Georges Clémenceau 91405 Orsay Cedex

<sup>b</sup>Laboratoire d'acoustique de l'université du Maine, Bât. IAM - UFR Sciences Avenue Olivier Messiaen 72085 Le Mans Cedex 9

<sup>c</sup>Institut des Nanotechnologies de Lyon - Site de l'UCBL, 6, rue Ampère 69621 Villeurbanne Cedex  
elie.lefeuvre@u-psud.fr

Today, microspeakers are used in many mobile electronics devices, such as mobile phones, tablets or MP3 players. Since 2009, this market exceeded one billion parts per year. However, in parallel to the sales increase, the performances of these small-size loudspeakers have been only very little improved in terms of sound quality, efficiency and power density over the last decade. Several reasons can explain such stagnation, such as the limits of conventional manufacturing techniques, or the focus put on selling points other than sound reproduction. The proposal made here is to take advantage of Micro-Electro-Mechanical Systems technologies for improving the microspeakers' performances. Indeed, such a technological leap appears as a promising way to overcome the major shortcomings of micro speakers made using conventional technologies. This paper shows, in the case of a novel structure of silicon microspeaker, some of the improvements which can be expected from MEMS technologies.

## 1 Introduction

The use of microspeakers has drastically grown over the past few years in reason of the important increase of mobile electronics devices having sound reproduction functions. Consumer electronics devices such as mobile phones, tablets or MP3 players are the most representative examples of everyday used devices with embedded microspeakers. Since 2009, this market exceeded one billion microspeakers per year. However, in parallel to the sales increase, the performances of these small-size transducers have been only very little improved in terms of sound quality, sound loudness and low energy consumption. This is mainly due to the integration requirements, which push towards a drastic reduction of the physical size of the microspeakers. To meet this requirement, the structure of the microspeakers is simplified, compared to usual large-size loudspeakers [1]. In particular, their diaphragm serves both as a sound radiator and as a suspension. This is far to be ideal from the acoustics point of view.

The proposal made here is to take advantage of Microsystems technologies for resolving the conflicting requirements of miniaturization and performances improvement. Such a technological leap appears actually as a promising way to overcome the major shortcomings of micro speakers made using conventional technologies.

Different studies have already demonstrated functional MEMS microspeakers [2-6]. However, these works focused on very small devices, below 25 mm<sup>2</sup> in area, capable of producing low Sound Pressure Level (SPL). Reported SPL were measured through a 2 cubic-centimeter coupler, typically used for the characterization of hearing-aid instruments, whereas SPL should be measured at 10 cm from the microspeakers, according to industrial standards for mobile applications.

Several actuation principles of MEMS microspeakers were investigated, such as electromagnetic [2-4], piezoelectric [5] and electrostatic [6]. Despite piezoelectric and electrostatic actuators are often considered as simpler than electromagnetic ones in terms of microfabrication and integration technologies, the latter has three major advantages regarding our application: high power density, low driving voltage and linear response. As the microfabrication of magnets having a high energy density remains difficult with today's technologies, in this work we considered the integration of a bulk magnet.

This paper presents the improvements enabled by MEMS technologies in the case of a novel structure of silicon microspeaker.

## 2 Design principles

The basic design principles of a microspeaker are similar to those of classic loudspeakers. Each part of the microspeaker, listed on the schematic structure represented in Fig. 1, has an influence on one or several characteristics of the electro-acoustic transducer. The main characteristics considered here are:

- the sound pressure level,
- the frequency bandwidth,
- the efficiency,
- the sound quality.

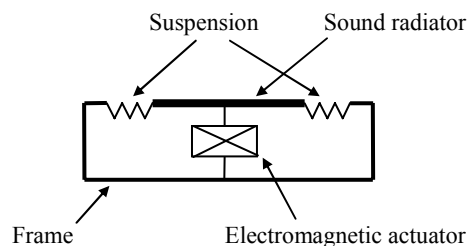


Figure 1: Schematic structure of the microspeaker

The acoustic wave is originated in the air by the out-of-plane displacement of the sound radiator, with an acoustic power  $P_{acoustic}$ . This power is related to the sound radiator surface (parameterized by the diameter  $d$  of the considered disc-shape radiator), the peak out-of-plane displacement  $x_{peak}$  and the frequency  $f$ , as expressed in (1) [7].

$$P_{acoustic} = 0.25d^4 f^4 x_{peak}^2. \quad (1)$$

The Sound Pressure Level  $L_{dB}$  quantifies the sound intensity perceived at the distance  $y$  from the sound radiator. Equation (2) gives the relation between the acoustic power, the SPL and the distance  $y$ .

$$P_{acoustic} = 10^{\frac{L_{dB}}{10}} \times 10^{-12} \times 4\pi \times y^2. \quad (2)$$

Thus, the choice of the sound radiator surface and its out-of-plane maximum displacement depend on two of the considered characteristics of the microspeaker: the targeted SPL and the frequency bandwidth. The expressions (1) and (2) clearly show that getting high SPL at low frequencies is conflicting with the reduction of the microspeaker sizes. To give some figures, in considering an acoustic intensity of 80 dB SPL at 10 cm distance from the sound radiator, the

corresponding volume of air displaced by the radiator is 11,1 mm<sup>3</sup>, 22.7 mm<sup>3</sup> and 124 mm<sup>3</sup> for the working frequencies of 1 kHz, 700 Hz and 300 Hz respectively.

The sound reproduction quality depends both on the linearity of the electro-mechanical actuator and the dynamic behavior of the sound radiator. As stated previously, the electromagnetic actuation is capable of good linearity. However, this property is not well optimized in most of the microspeakers used in mobile electronic devices. Concerning the sound radiator, its dynamic behavior should be ideally similar to a piston. In particular, all its structural modes should be set out of the frequency bandwidth. Indeed, the presence of structural resonances induces phase and amplitude distortion of the radiated sound wave. The resonance frequency of the spring-mass system, composed of the suspension stiffness and the mass of the mobile part, should be set at a frequency below the lower limit of the frequency bandwidth. The other vibration modes of the sound radiator should be ideally set at frequencies higher than the upper limit of the frequency bandwidth. However, this is difficult in practice for several reasons. The main limitations come from the wide considered bandwidth and from the difficulty to get a light and stiff sound radiator part. Conic and dome shapes are used in loudspeakers to address this problem, but they cannot be that effectively implemented in the case of microspeakers because of restricted dimensions.

The electro-acoustic efficiency  $\eta$  of the microspeaker depends on the design of the electromagnetic actuator and on the mass of the mobile part. It can be expressed as follows [7]:

$$\eta = \frac{\rho \cdot \pi \cdot r^4}{4c} \cdot \frac{1}{R} \cdot \left( \frac{f_{Force}}{M_{mobile}} \right)^2 \quad (3)$$

In (3),  $\rho$  represents the air density,  $r$  the radius of the disc-shaped acoustic radiator,  $c$  the sound speed,  $R$  the coil resistance, and  $f_{Force}$  the force factor of the electromagnetic actuator. The electromagnetic design, not detailed in this paper, includes an NdFeB permanent magnet attached to the frame and a copper microcoil attached to the mobile part. The mobile mass  $M_{mobile}$  can be considered as the sum of the mass of the acoustic radiator and mass of the microcoil. According to (3), the mobile mass should be as small as possible to maximize the efficiency. So, the radiator mass should be minimized. However, this point is conflicting with the objective of high stiffness for the acoustic radiator, so that a piston-like motion is obtained over the whole frequency bandwidth.

In the next section, the properties of different materials are examined in order to find the best trade-off between lightness and stiffness of the acoustic radiator, which remains today a major technical lock regarding the efficiency and the sound quality of the microspeakers.

### 3 Sound radiator

A disc-shaped plate was chosen here for the sound radiator. Oval and rectangular shapes are commonly used for improving the integration of the microspeakers. However, setting structural modes out of the frequency bandwidth is more difficult in these two last cases.

The plate surface was determined with the help of (1) and (2) in considering an acoustic intensity of 80 dB SPL at

10 cm distance from the sound radiator, and a 300 Hz to 20 kHz frequency bandwidth. This led to consider the diameter  $d$  of 15 mm and the maximum peak displacement  $x_{peak}$  of 300  $\mu$ m as a good trade-off regarding the integration constraints and the microfabrication possibilities.

As several materials other than silicon could be used for the sound radiator, we defined first a figure of merit to make the choice easier. This figure of merit was defined in considering the material properties, which determines the mass and the modal frequencies of the disc-shaped sound radiator. For a free disc-shaped plate, the modal frequencies can be computed using the following analytical expression:

$$f_i = \frac{2}{\pi} \cdot \left( \frac{\beta_i}{d} \right)^2 \cdot \sqrt{\frac{E}{\rho} \cdot \frac{h^2}{12(1-\nu^2)}} \quad (4)$$

In (4),  $\beta_i$  is the characteristic constant of the mode  $i$ ,  $d$  the disc diameter,  $h$  its thickness,  $E$  the Young's modulus,  $\rho$  the material density, and  $\nu$  the Poisson coefficient [9]. Eq. (4) shows that the modal frequencies depend on the  $E/\rho$  ratio and the thickness  $h$  of the disc. For our application, the lowest modal frequency,  $f_1$ , should ideally be higher than 20 kHz. Whereas the mass  $M$ , which depends on the disc thickness  $h$  and the material density  $\rho$ , should be as small as possible. Using (4), it is possible to substitute  $h$  in the expression of the disc mass  $M$ . This leads to the following expression of  $M$ :

$$M = \frac{\pi^2 \cdot d^4 \cdot f_1}{8\beta_1} \cdot \sqrt{12 \cdot \frac{\rho^3}{E} \cdot (1-\nu^2)} \quad (5)$$

According to (5), for fixed values of  $d$ ,  $f_1$  and  $\beta_1$ , the  $E/\rho^3$  ratio should be as high as possible in order to minimize the mass  $M$ . This ratio was chosen as a figure of merit for selecting the membrane material. The Poisson coefficient was not taken into account due to its second-order influence. It should be noted that other boundary conditions and other geometries, such as free and clamped rectangular plates, lead to the same expression of the figure of merit.

Table 1: Figure of merit of different materials.

Material	$\rho$ (gr/cm <sup>3</sup> )	E (GPa)	$E/\rho^3$
C (Diamond)	3.52	1000	22.9
Si	2.33	165	13.0
SiO2	2.2	107	10.0
Mg	1.74	45	8.54
Al2O3	3.97	390	6.23
Al	2.7	69	3.50
Ti	4.54	115	1.22
Polyimide	1.43	3.2	1.09
Cr	7.19	298	0.80

The figure of merit of different materials was calculated and summarized in Table 1. As one can notice, except for diamond, the silicon material has the highest figure of merit. Moreover, this material presents the advantage of having a large panel of micromachining processes available.

Once the silicon material selected, the thickness of the disc was computed in order to set the modal frequencies above 20 kHz. This led to a thickness of 320  $\mu\text{m}$  and a mass of 132 mg. Smaller thicknesses were investigated to make the membrane lighter, but FEM simulations and analytical expressions confirmed that a lot of modal frequencies were inside of the frequency bandwidth. For instance, with a disc thickness of 20  $\mu\text{m}$ , the mass is 8 mg only, but 30 modes are in the frequency bandwidth, as summarized in Table 2.

To find a better trade-off mass and rigidity, we have studied the design of the microstructure represented in Fig. 2. This microstructure is composed radial and circular ribs etched in one side of the 320  $\mu\text{m}$  thick silicon disc. The ribs thickness is 300  $\mu\text{m}$ , so that the sound radiator minimum thickness is 20  $\mu\text{m}$ . Structures with various number of ribs and different ribs width were analyzed using FEM simulations. The best trade-off was obtained for a middle ring of 9.7 mm in diameter and 200  $\mu\text{m}$  in width, and 8 inner and 12 outer ribs of 100  $\mu\text{m}$  width. According to the simulation results, the structural modes are in this case limited to just two in the microspeaker frequency bandwidth: the first one at 8.52 kHz and the second one at 15.38 kHz. The mass of this optimized silicon sound radiator is 24 mg, that is to say 5.5 times lighter than the 320  $\mu\text{m}$  thick silicon disc of the same 15 mm diameter. This mass reduction has a huge impact on the electro-acoustic efficiency. Indeed, according to (3) a mass reduction by a factor 5.5 roughly increases the efficiency by a factor 30.

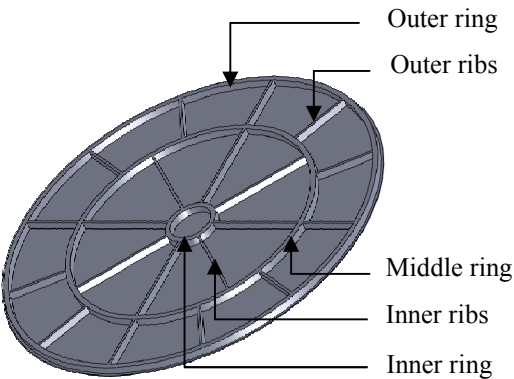


Figure 2: Microstructure of the silicon sound radiator

Table 2: Mass and modal characteristics for different designs of the sound radiator.

Sound radiator design	Membrane mass (mg)	Drum mode frequency (kHz)	Number of modes between 300 Hz and 20 kHz
10 $\mu\text{m}$ thick disc	4	0.62	50
20 $\mu\text{m}$ thick disc	8	1.32	30
320 $\mu\text{m}$ thick disc	132	20.15	1
Microstructured disc	24	15.38	2

The experimental validation of the design was performed by vibration analysis of the microstructured

silicon discs. The signature of the two vibration modes was observed at frequencies of nearly 8.8 kHz and 17.9 kHz, as show on Fig. 3. The discrepancy between FEM simulations and measurements are probably partly due to the inaccuracy of the material properties used in the FEM modeling. In the experimental setup, the microstructured silicon disc was suspended by a series of soft suspension springs, which slightly differs from the free boundary conditions used in the FEM simulations.

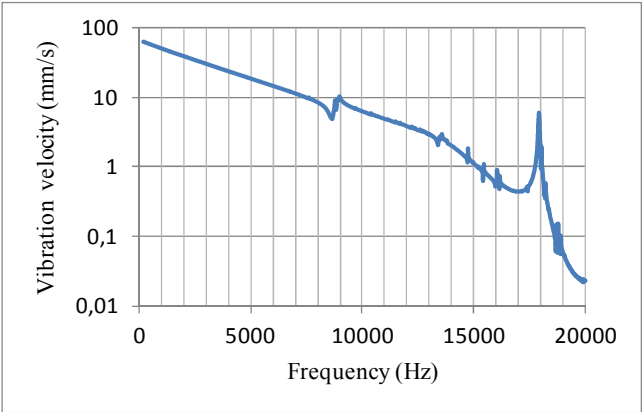


Figure 3: Experimental vibration velocity spectrum of the microstructured silicon sound radiator

#### 4 Suspension

According to the trade-off found between the sound radiator diameter and its maximum out-of-plane displacement presented in the previous Section 3, the suspension should enable a displacement of 300  $\mu\text{m}$  at least. For this part of the microspeaker also, silicon material presents several advantages. Indeed, this single crystal has an outstanding resistance to mechanical fatigue. Moreover, thanks to micromachining technologies, it is possible to design very soft springs, in spite of high Young's modulus of silicon.

Compared to the displacements usually considered in MEMS, no larger than a few microns, the 300  $\mu\text{m}$  maximum displacement required for this application can be considered as a real challenge. The four different suspension structures, which were designed using FEM simulations, are depicted in Fig. 4. The thickness of the silicon springs is 20  $\mu\text{m}$ . Their rounded shapes were conceived with the objective of minimizing the mechanical stress, located near the anchorages, in order to insure good reliability of the device. For 300  $\mu\text{m}$  out-of-plane displacement, maximum principal stress of 28 MPa, 46 MPa, 20 MPa and 36 MPa were computed for the structures a, b, c and d respectively. These values are very far from the elastic limit of silicon material, commonly considered as 7 GPa in (111) crystalline direction.

The stiffness of the suspension was set so that the piston mode frequency of the device occurs at frequencies lower than 300 Hz. FEM modal analyses of the sound radiator and the four different suspension structures predicted that the piston mode frequency takes place at frequencies comprised between 35 Hz and 85 Hz.

The four suspension structures were microfabricated and tested in order to verify their robustness and their linearity. Static testing showed that they could stand more

than 4 mm out-of-plane displacement. It is much more than required in normal working conditions, but this ensures an appreciable large safety margin. Fig. 5 shows the experimental characteristics of force a function of the out-of-plane displacement of the four suspension structures. These results confirmed the stiffness values predicted by the FEM simulations. The suspensions structures (a) and (c) have almost the same stiffness of nearly 2 N/m, whereas the structures (b) and (d) exhibit a stiffness of approximately 5 N/m.

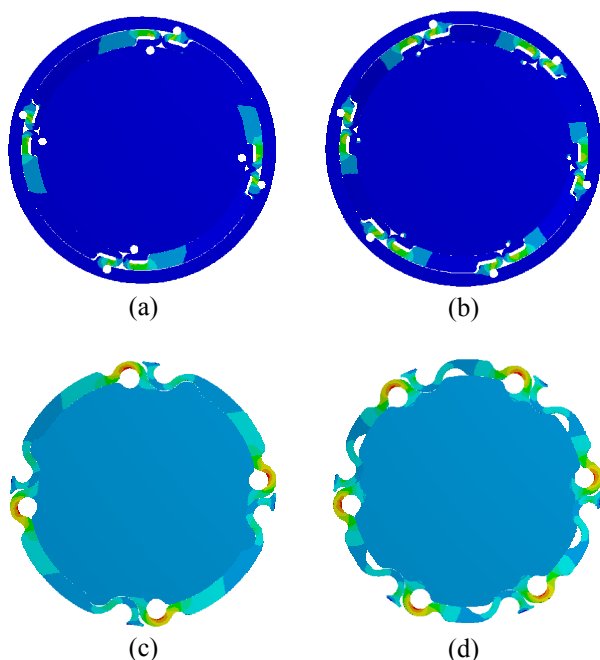


Figure 4: Stress distribution in the four suspension structures, for 300  $\mu\text{m}$  out-of-plane displacement

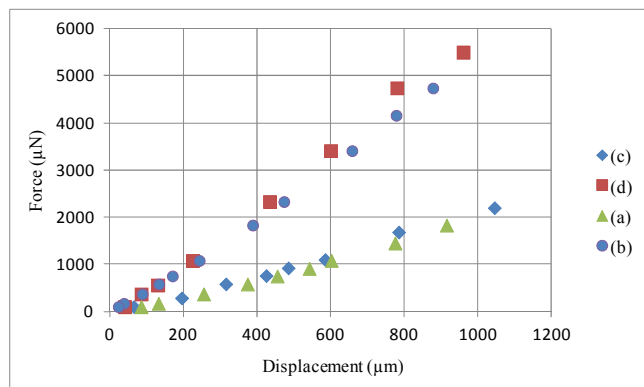


Figure 5: Experimental characteristics of force vs. displacement for the (a), (b), (c) and (d) suspension structures

## 5 Conclusion

This paper presented first the design principles followed to elaborate a MEMS microspeaker with high performances. The objectives were to get a sound pressure level of 80 dB at 10 cm high in the 300 Hz – 20 kHz frequency bandwidth. High electro-acoustic efficiency and high sound quality were also considered as priorities for this work. These two latter characteristics depend strongly

on the mass of the sound radiator and its dynamic behavior. Starting from these observations, a figure of merit of the material used for the sound radiator was proposed. This figure of merit showed that, apart the diamond, the silicon material was of major interest for this application because of its low density and its high Young's modulus. Then, taking advantage of the MEMS micromachining possibilities, an innovative silicon-based sound radiator was designed and optimized using FEM simulations. Vibration tests performed on the microfabricated samples confirmed the effectiveness of the design, with only two modal frequencies in the considered audio bandwidth.

Silicon material exhibited also very good properties for the suspension of the sound radiator. Indeed, this single-crystal material is very resistant to mechanical fatigue. However, the challenge was to reach out-of-plane displacements as important as 300  $\mu\text{m}$ , much larger than usual MEMS displacements. This very large out-of-plane displacement resulted from the high sound pressure level targeted. This objective was reached by the design of a set of suspension springs with particular shapes, optimized using FEM simulations to have a good distribution of the mechanical stress.

Thus, this work proposed an innovative approach, based on the Micro-Electro-Mechanical-Systems Technologies, to overcome the main technical limitations of today's microspeakers. This was successfully demonstrated in this paper for two important parts of a microspeaker, the sound radiator and the suspension. Besides, the design of the electromagnetic actuator of the microspeaker could profit as well from the MEMS technologies.

## Acknowledgments

This work was financially supported the French National Research Agency (ANR).

## References

- [1] M. R. Bai, C.-Y. Liu, R.-L. Chen, "Optimization of Microspeaker Diaphragm Pattern Using Combined Finite Element–Lumped Parameter Models", *IEEE Trans. Mag.*, 44(8), 2049-2057 (2008)
- [2] Y. C. Chen, and Y. T. Cheng, "A low-power milliwatt electromagnetic microspeaker using a PDMS membrane for hearing aids application", in *Proc. MEMS*, 1213-1216 (2011)
- [3] S. S. Je, F. Rivas, R. E. Diaz, J. Kwon, J. Kim, and B. Bakkaloglu, "A compact and low-cost MEMS loudspeaker for digital hearing aids", *Trans. Biomed. Circ. and Syst.*, 3(5), 348-358 (2009)
- [4] M. C. Cheng, W. S. Huang, and S. R. S. Huang, "A silicon microspeaker for hearing instruments", *J. Micromech. Microeng.*, 14, 859-866 (2004)
- [5] S. H. Yi and E. S. Kim, "Micromachined piezoelectric microspeaker", *Jap. J. of App. Phys.*, 44(6A), 3836-3841 (2005)
- [6] H. Kim, A.A. Astle, K. Najafi, L.P. Bernal, P.D. Washabaugh, F. Cheng, "Bi-directional Electrostatic Microspeaker with Two Large-Deflection Flexible Membranes Actuated by Single/Dual Electrodes", *In Proc. IEEE Sensors 2005*, 89-92 (2005)
- [7] I. Shahosseini, E. Lefeuvre, M. Woytasik, J. Moulin, X. Leroux, S. Edmond, E. Dufour-Gergam, A. Bosseboeuf, G. Lemarquand, and V. Lemarquand, "Towards high fidelity high efficiency MEMS microspeakers," in *Proc. IEEE Sensors*, 2426-2430 (2010)
- [8] I. Shahosseini, E. Lefeuvre, E. Martincic, M. Woytasik, J. Moulin, S. Megherbi, R. Ravaud, G. Lemarquand, "Design of the silicon membrane of high fidelity and high efficiency MEMS microspeaker," in *Proc. DTIP'2011* (2011)
- [9] J.S. Rao, *Dynamics of plates*, Narosoa Publishing House Ed. (1999)